recycling

MDPI

Article

Microstructural and Thermal Behaviour of Composite Material from Recycled Polyethylene Terephthalate and Fly Ash

Nur Hazzarita Mohd Nasir [1,*], Fathoni Usman [2], Ean Lee Woen [2], Mohamed Nainar Mohamed Ansari [3], Abu Bakar Mohd Supian [2] and Saloma [4]

[1] College of Graduate Studies, Universiti Tenaga Nasional (UNITEN), Kajang 43000, Malaysia
[2] Institute of Energy Infrastructure, Universiti Tenaga Nasional (UNITEN), Kajang 43000, Malaysia
[3] Institute of Power Engineering, Universiti Tenaga Nasional (UNITEN), Kajang 43000, Malaysia
[4] Department of Civil Engineering, Faculty of Engineering, Universitas Sriwijaya, Palembang 30128, Indonesia
* Correspondence: sc23286@student.uniten.edu.my

Abstract: Nowadays, the environmental impact of plastic waste is crucial, and in the energy industry, fly ash, a type of solid waste, has also prompted severe ecological and safety concerns. In this study, we synthesised composite material from two industrial wastes: recycled polyethylene terephthalate (rPET) as the matrix and fly ash as the filler. The effect of different fly ash loadings on the thermal behaviour and microstructure of the composite material using rPET were evaluated. Various loading amounts of fly ash, up to 68%, were added in the rPET mixtures, and composites were made using a single-threaded bar's barrel extruder. The feeding zone, compression zone, and metering zone made up the three functional areas of the extruder machine with a single-flighted, stepped compression screw. The composite materials were subjected to DSC and SEM equipped with EDX spectroscopy tests to examine their thermal behaviour and microstructural development. It was found that the thermal behaviour of rPET improved with the addition of fly ash but degraded as the fly ash loading increased to 68%, as confirmed by the DSC study. The composites' microstructural development revealed an even filler distribution within the polymer matrix. However, when the fly ash loading increased, voids and agglomeration accumulated, affecting the composites' thermal behaviour.

Keywords: energy; composite material; recycled PET; fly ash; polymer; thermal behaviour; microstructure

Citation: Mohd Nasir, N.H.; Usman, F.; Woen, E.L.; Ansari, M.N.M.; Supian, A.B.M.; S. Microstructural and Thermal Behaviour of Composite Material from Recycled Polyethylene Terephthalate and Fly Ash. *Recycling* **2023**, *8*, 11. https://doi.org/10.3390/recycling8010011

Academic Editor: Dariusz Mierzwiński

Received: 8 November 2022
Revised: 3 January 2023
Accepted: 4 January 2023
Published: 9 January 2023

1. Introduction

The amount of plastic produced worldwide increased dramatically from 2 million tonnes in 1950 to 367 million tonnes in 2020 [1,2]. There were 9.2 billion tonnes of plastic produced between 1950 and 2017, which is more than a tonne for every person on the globe today [3], whereas only 600 million tonnes have been recycled [1]. In addition to being lightweight and easy to shape, plastic is exceptionally resilient. A wide range of industrial items can benefit from these properties, including the textile, automotive, manufacturing, construction, aerospace, and packaging industries [4–10], but the majority of plastic, over 40%, is used for packaging. Polyethylene terephthalate (PET) is impermeable to gases and liquids and is the dominant material used to manufacture beverage bottles. PET production capacity worldwide surpassed 30.5 million metric tonnes in 2019, and this number is forecast to increase to 35.3 million metric tonnes by 2024 [11]. It is also one of the most commonly found regular plastics in landfills worldwide, primarily from mineral water and carbonated beverage bottles. PET has excellent mechanical strength, chemical resistance, clarity, transparency, processability, colourability, and good thermal stability [12]. Therefore, PET recycling is one of the most widely used polymer waste recycling methods [13]. As a result, researchers all around the world are working hard to find opportunities to turn PET waste into high-value raw materials and other beneficial products [12,14–19].

Meanwhile, Malaysia is powered by coal, which accounts for 43% of its energy [20], burning 33.4 million metric tonnes of coal in 2019 [21], approximately 92% of which came

from foreign nations, including Indonesia (73.8%) and Australia (17.9%) [22]. Malaysia was not among the 40 countries that pledged to phase out coal use by 2030 or 2040 at the November COP26 climate meeting [23]. Coal appears to be and will continue to be a significant energy source in the country. While this may be beneficial to the industries' bottom lines in the short term, it may be detrimental to everyone in the long run. The electric power stations that burn coal produce fly ash as a waste by-product. Fly ash is a spherical fine glass powder with a particle size estimated to range from 0.5 to 100 µm and comprises heterogeneous material where SiO_2 (silicon dioxide, silica), Al_2O_3 (aluminium oxide), Fe_2O_3 (iron oxide), and occasionally CaO (calcium oxide) are the main chemical components [24]. Fly ash containing a SiO_2 + Al_2O_3 + Fe_2O_3 content between 50 and 70% and low in lime (CaO < 18%) is defined as class F, and fly ash high in lime (CaO > 18%) is defined as class C according to the American Society for Testing Materials (ASTM C618-19) [25]. Class F fly ash produced from burning harder, older anthracite and bituminous coal has a high silicate and low calcium content. Class C fly ash has a low silicate and high calcium concentration produced from burning younger lignite or sub-bituminous coal.

Until now, coal-fired power plants have buried or returned trash from their equipment to strip mines to dispose of it [26]. However, fly ash can be converted into a valuable and useful product if appropriately utilised. Many studies have been conducted to increase the utilisation of fly ash in geotechnical applications, including soil stabilisation for roads, mine fill, trenches, retaining walls, landfill liners or covers, and geopolymer materials [27,28]. Fly ash is also an excellent filler material for polymers due to its density, superior dispersibility, and fluidity of spherical particles, and there has been growing attention paid to its utilisation as a filler [29–49]. According to Sreekanth et al. [48], in particulate-filled polymer composites, the mechanical characteristics are influenced by the size, shape, distribution, and adherence of the filler particles in the matrix polymer. The crystallisation and degree of crystallinity of a semicrystalline polymer affect the physical and mechanical properties of a polymer product [50].

Fa et al. [51] studied the crystallisation behaviour of different blow-moulded PET bottles, showing differences in crystallisation behaviours. The decrease in crystallisation temperature (T_c) during heating demonstrates a close relationship between the onset of crystallisation during heating and the subsequent crystallisation behaviour during cooling. Furthermore, less energy is required for amorphous fraction relaxation, which may induce further crystallisation via DSC heating, indicating ease of crystallisation from the glassy state [51].

Rebeiz et al. [39] produced polymer mortar (PM) from recycled PET and fly ash, and DSC was used to analyse the effect of fly ash on PM's glass transition temperature (T_g). Fly ash concentrations ranging from 0% to 25% do not affect polyester's 30 °C glass transition temperature [39]. David, in [38], conducted DSC investigations in the heating (endothermic) and cooling (exothermic) modes to further investigate the crystalline behaviour of the composite material rPET with 0–44% fly ash. The result shows that the melting temperature (T_m) of the composite material with increased fly ash loading was higher than that of the composite material with low fly ash concentrations due to its crystalline component and more orderly molecular structure. The inclusion of fly ash in the composite material increases the crystallisation temperature (T_c) because it reduces the rate at which the material is cooled during production.

Mohsin et al. [52] used DSC to analyse PET waste water bottles treated with ethylene glycol (EG) using a reactive extrusion process. PET's melting point decreased from 250.08 °C to 242.33 °C when the EG mass was increased from 0.4 to 2 g. This decrease in melting temperature indicated that EG affected PET molecules' orderly compact arrangement, improving PET segment mobility and minimising crystalline areas [52].

In this paper, the effect of fly ash used as a filler in recycled PET to produce composite material using an extrusion process was evaluated through DSC and SEM/EDX to achieve a better understanding of the effect of fly ash loading on the thermal behaviour, including crystallisation and melting transition. The SEM image results validate our finding on the

filler distribution in the microstructure of the composite material. The current research will aid in developing fly ash–rPET composite materials and provide information on the recycling and reuse of fly ash and PET waste products.

2. Results

Figure 1 illustrates the thermograms from differential scanning calorimetry (DSC) that were used to compute the glass transition temperature (T_g), peak melting temperature (T_m), peak cooling crystallisation temperature (T_c), and the melting enthalpies (ΔH_m), which are summarised in Table 1.

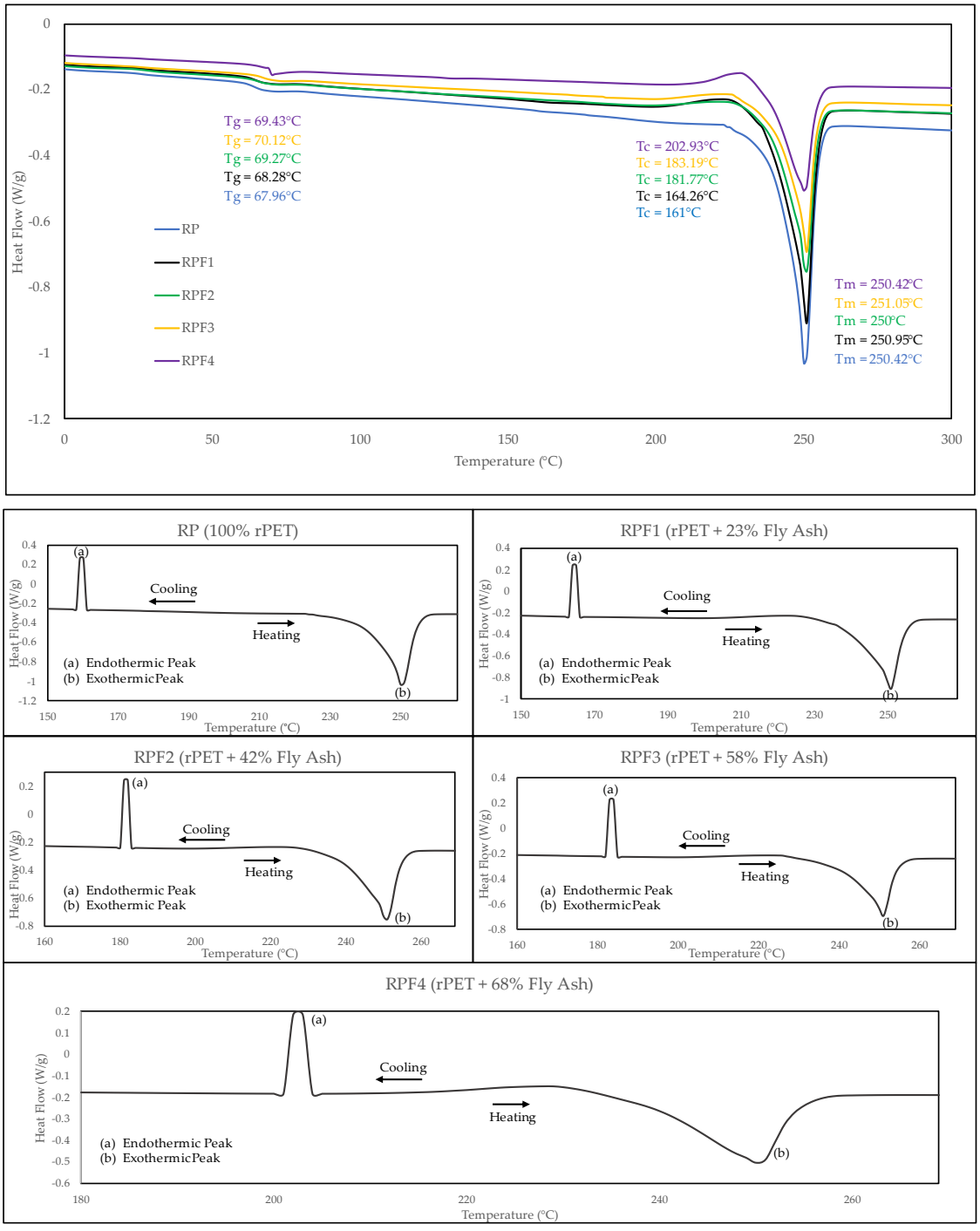

Figure 1. DSC thermograms of 100% rPET (RP), rPET with 23% fly ash (RPF1), rPET with 42% fly ash (RPF2), rPET with 58% fly ash (RPF3), and rPET with 68% fly ash (RPF4).

Table 1. Thermal profile of the composite material rPET–fly ash.

FLY ASH (%)	TG (°C)	TC (°C)	TM (°C)	ΔHM (J/G)	χC (%)
0	67.96	161.00	250.42	42.70	30.5
23	68.28	164.26	250.95	39.75	28.4
42	69.27	181.77	250.65	30.67	21.9
58	70.12	183.19	251.05	26.72	19.1
68	69.43	202.93	250.42	22.40	16.0

It can be seen from Table 1 that the glass transition temperature, T_g, increased with the increase in fly ash content from 23% to 58% and slightly decreased for a fly ash loading of 68%. The highest Tg achieved was 70.12 °C with 58% fly ash loading. This shows that fly ash affects the glass transition temperature of rPET, which is different from what has been found by Rebeiz et al. [39] and Cazan et al. [16]. Their findings show that fly ash has an insignificant effect on the glass transition temperature. Fly ash makes the rPET glassy state more stable, making breaking the polymer chain difficult. Therefore, the glass transition temperature increases because more energy is required to break the chains. The cooling crystallisation temperature, T_c, of the composite material also increases. The increase in fly ash content from 23% to 68% led to a peak crystallisation at 202.93 °C with 68% fly ash loading. The result follows David's [38] earlier finding that the fly ash concentration in the composite material correlates with the rPET peak crystallisation cooling temperature. The addition of fly ash to the composite material increases T_c because it slows the rate at which the material cools during production. The melting temperature, T_m, of rPET is 250.42 °C. T_m increased with greater amounts of fly ash loading, and the highest T_m recorded was 251.05 °C with 58% fly ash loading. This shows that fly ash influences crystallinity in rPET. As the crystalline structure becomes more ordered, T_m increases. However, at 68% fly ash loading, the T_m decreased to 250.42 °C, resulting from the disordered structure due to the high fly ash loading.

These findings show that the filler loading significantly affected the T_g and T_c, as reflected by r values of 0.811 and 0.87, respectively, and a *p*-value of less than 0.05 from the statistical analysis. However, the filler loading was less affected by the T_m, as reflected by an r value of 0.17 and a *p*-value greater than 0.05.

Meanwhile, a decrease in the melting enthalpy ΔH_m was noticed with the increase in fly ash loading. The rPET material had the highest ΔH_m, 42.70 J/g, and the composite material with 68% fly ash had the lowest ΔH_m, 22.40 J/g. The calculated crystallinity degree (Xc) from Equation (1) shows that the crystallinity degree (Xc) decreased in response to the melting enthalpy ΔHm because rPET chains cannot be packed tightly. This also suggests that the filler and matrix are compatible [53], proving that adding fly ash lowers the latent heat necessary for melting rPET from its solid state to its liquid form.

3. Discussion

Figure 2a shows the surface SEM image of continuous matrix rPET, and the EDX analysis shows the presence of O and S, and no impurities were detected on the rPET matrix. The EDX analysis in Figure 2b–e revealed the presence of O, Al, and Si as the main elements with a small amount of Mg, S, Ca, Fe, and K. These elements are derived from the source material of fly ash. With the inclusion of fly ash in the polymer matrix, the dispersion of fly ash particles inside the polymer matrix was evident, as shown in the SEM image from Figure 2b–e. However, voids and agglomeration were noticed, resulting from fly ash particles inadequately bonding with the rPET matrix. Fly ash additions of up to 68% resulted in a rougher polymeric matrix, and the composite systems with fly ash contents of 58 and 68% had more voids and agglomerated non-interlocking sites than the other samples (Figure 2d,e). This shows the polymer matrix lost its fly ash absorption ability, confirming poor fly ash and rPET matrix bonding at increased filler loading amounts. The brittleness of the composite structure increased as the likelihood of fly ash aggregation increased. Figure 2e shows an aggregation of fly ash with a higher loading percentage but

insufficient encapsulation by the rPET matrix. As a result, particles agglomerated within the polymer matrix at higher fly ash loadings, causing the matrix to fail. The deformability of the composites was decreased due to the increase in the fly ash loading.

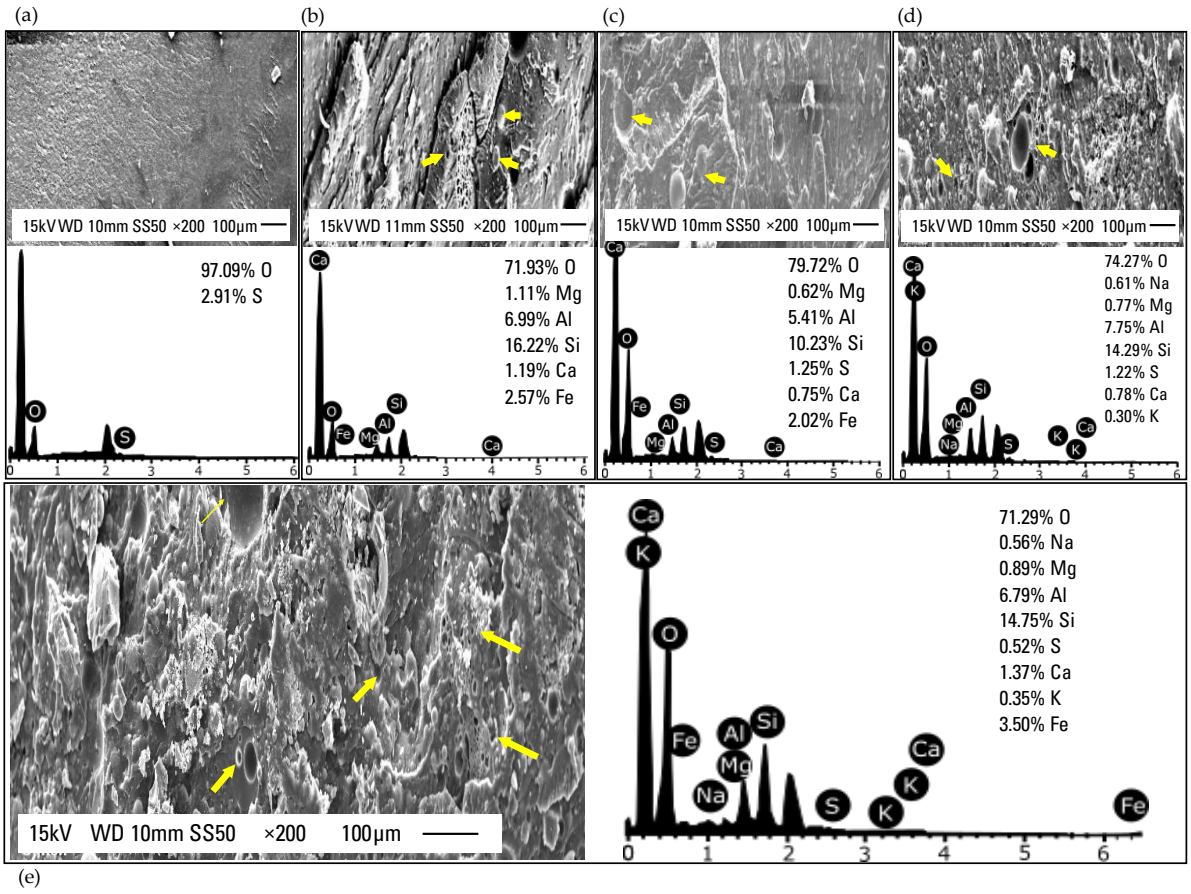

Figure 2. SEM and EDX analysis for (**a**) RP, (**b**) RPF1, (**c**) RPF2, (**d**) RPF3, (**e**) RPF4. The yellow arrows show the particle agglomerates and voids.

Figure 3a,b shows the surface SEM image of composite materials with 23% and 68% fly ash before they were pelletised into small granules using a shredder machine (non-shredded). Figure 3a shows that fly ash agglomeration occurs in a minimal condition, while Figure 3b shows that significant and close agglomeration occurred. This is consistent with the SEM findings in Figure 2b,e, where agglomeration can be seen to increase with the amount of fly ash in the composite. However, the sample that was non-pelletised exhibited a sharper SEM image. This shows that the rough and ruptured SEM images in Figure 2b–e were caused by a micro-tear defect in the samples generated by the shredding process.

The above findings show that the filler loading affects the thermal behaviour and microstructure of rPET–fly ash composite material. Tg, Tc, and Tm increased as the fly ash loading increased from 23% to 58%, indicating that particle bonding between the filler and matrix improved the thermal behaviour of the composite material. However, adding up to 68% fly ash results in a reduction in the Tg and Tm of the composite material. This indicates that the particle bonding of the matrix with the highest filler loading weakened, affecting the thermal behaviour. SEM analysis also supports composite materials with 68% fly ash loading having a microstructure filled with agglomeration, voids, and cracks. The particle bonding between rPET and fly ash reached its optimum thermal profile results with a fly ash loading of up to 58%. In summary, the constituents of the rPET–fly ash composite tend to aggregate, leading to separated phases and inhomogeneous blends with poor interphase adhesion, which affect the thermal behaviour and reduce the performance of the composite

material. Thus, compatibility approaches must be developed to improve the adhesion between rPET–fly ash, improving the composite materials' ultimate properties.

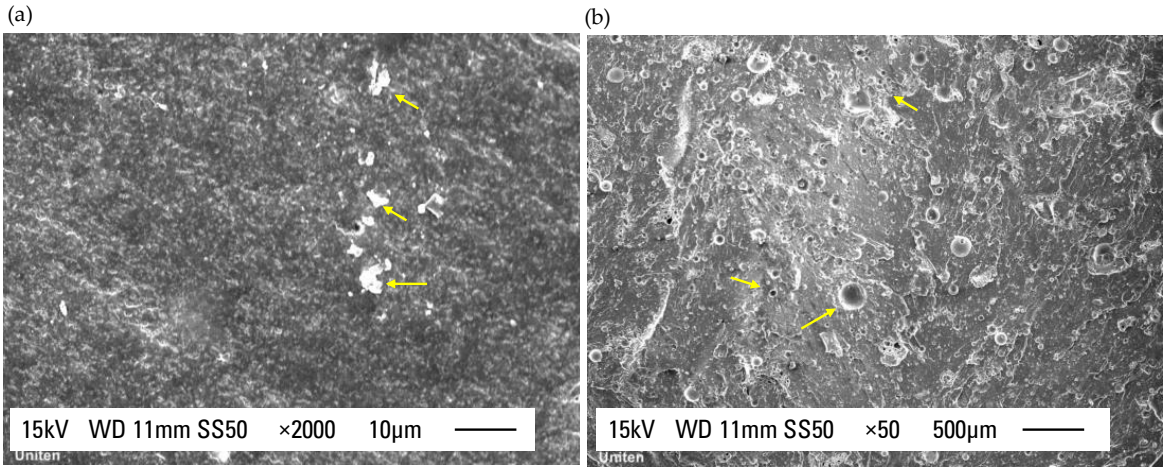

Figure 3. SEM analysis for (non-shredded samples) (**a**) RPF1, (**b**) RPF4. The yellow arrows show the particle cracks and agglomerates.

4. Materials and Methods

4.1. Main Materials

The waste PET shown in Figure 4 was collected in the form of beverage bottles from integrated recycling facilities (IRFs), in Putrajaya. Physically removing the bottle caps, labels, and adhesives from PET bottles was the first step in preparing them for processing. The PET bottles were then shredded into flaky fragments using a shredder machine as part of a mechanical recycling process and then rinsed in water to eliminate any residues and contaminants.

PET bottles collected at IRF	Bottle caps, labels and adhesives were removed	rPET was shredded into flakes

Figure 4. The collection and processing of recycled PET (rPET).

The characterisation of rPET flakes was analysed with X-ray fluorescence (XRF) analysis and Fourier transform infrared spectroscopy (FTIR) for chemical element composition. The chemical elements traced by XRF (Shimadzu Corporation, Tokyo, Japan) for rPET were SO_3 (53.715%), K_2O (37.417%), CuO (4.845%), and FE_2O_3 (4.023%), which were prob-

ably from additive agents such as flame retardants, stabilisers, and oxidants during the manufacturing process [5,12,54–57] and also due to the contamination [12,58].

Figure 5 illustrates the Fourier transform infrared (FTIR) (TA Instruments, DE, USA) spectra of rPET flakes and the FTIR list of functional groups shown in Table 2. The absorption bands of rPET were detected at 2966 cm^{-1} (C H stretching) and 1713 cm^{-1} (C=O stretching), representing carboxylic acid; 1578 and 1504 cm^{-1} (C=C stretching), representing the aromatic ring; and 1242 and 1095 cm^{-1} (–O– stretching), representing the terephthalate group. The CO_2 peak was detected at 723 cm^{-1}. Based on the spectra library listing, potential substances of polyethylene terephthalate (PET) with an index number of 57 hit 95%, and polyester with an index number of 32 hit 92.74%. Another outstanding absorption of PET and isophthalic acid with an index number of 23 hit a 67% match, which indicated the presence of additives used in the manufacture of PET bottles, as validated by the XRF result. In addition, the detection of common elements such as an adhesive (index no. 228), denim (index no. 34), and inkjet (index no. 28) hit matches of 93%, 81%, and 79%, respectively.

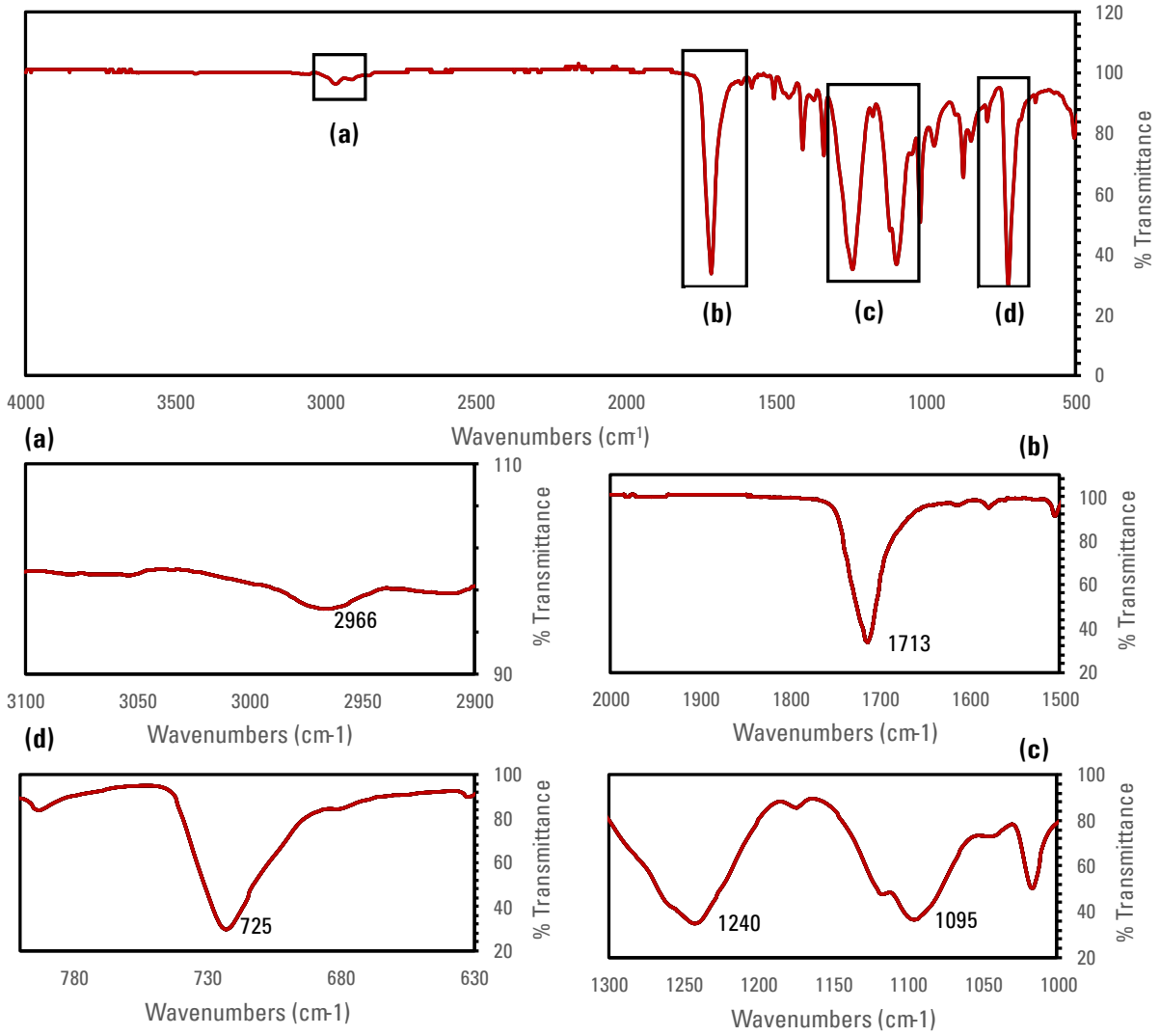

Figure 5. FTIR spectra peak values for rPET, which were detected at the following wavenumbers: (**a**) 2966 cm^{-1} for CH bond; (**b**) 1713 cm^{-1} for CO bond; (**c**) 1240, 1095 cm^{-1} for O bond; (**d**) 25 cm^{-1} for CO_2 bond.

Table 2. Specific functional groups' FTIR absorption wavenumbers.

Name	Location of Absorption Curve (cm^{-1})	Corresponding Species and Functional Groups	Vibration Types
CH	2966	C H	Stretching
C=O	1713	Carboxylic acid group	Stretching
C=C	1578 1504	Aromatic ring	Stretching
–O–	1242 1095	Terephthalate group	Stretching
CO_2	723	C=O	Stretching

The fly ash was obtained from the Jimah Power Plant and was dried in the oven for 24 h (100 °C). The filler size ranged from 45 to 170 µ. The XRF analysis in Table 3 shows that the total element content of SiO_2 and Fe_2O for fly ash was 73.29%, and its Ca content was 13.657%, so the fly ash was classified as class F in accordance with ASTM C618-19 [25].

Table 3. The chemical composition of the fly ash.

SiO_2	Fe_2O_3	CaO	K_2O	TiO_2	BaO	SrO	SO_3	ZrO_2
41.877	32.413	13.657	3.263	3.234	1.622	1.617	1.066	0.455

Figure 6 shows the outcomes of an investigation using SEM/EDX (Joel, Tokyo, Japan) to study the particle shape of fly ash. It can be seen that the fly ash particles were almost amorphous spheres with over 90% chemical proportions of oxygen (O), silica (Si), and aluminium (Al) in high signal intensities, which is known as an amorphous alumina silicate sphere [24]. In contrast, the relatively weak signal intensities in sodium, magnesium, sulphur, calcium, potassium, iron, titanium, and zirconium indicated lower particle concentrations in these elements. However, this signal cannot be used to conclude the percentage of chemical content as stated in XRF analysis but only shows the signal intensities of the elements.

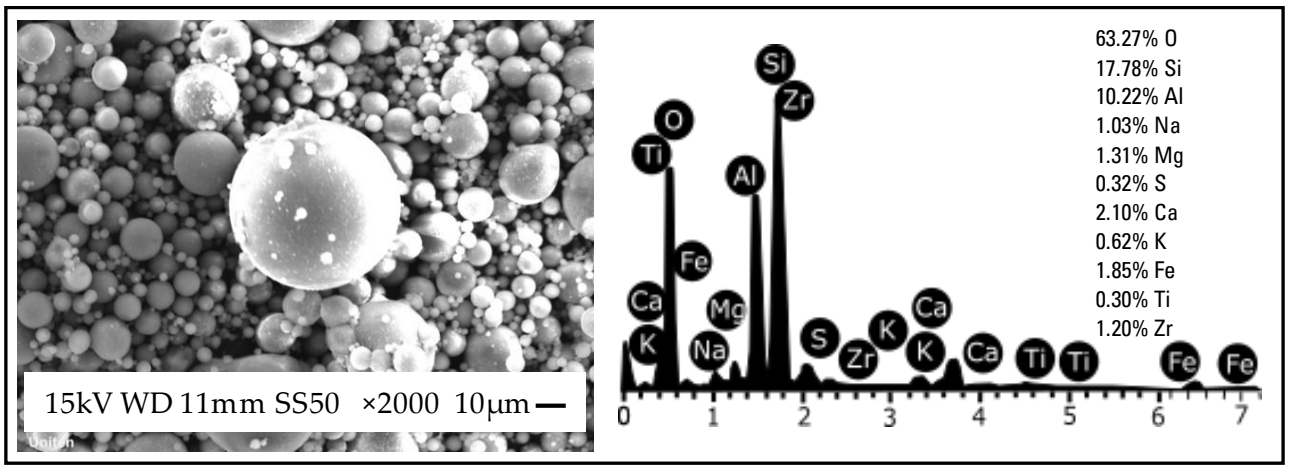

Figure 6. The SEM and EDX analysis of fly ash.

4.2. Sample Preparation

PET waste bottles were fragmented to a size of 3–10 mm and then mixed with fly ash at 23, 42, 58, and 68% by dry weight, as presented in Table 4. The control sample, containing rPET only (0% fly ash), is labelled as RP, while RPF1 to RPF4 indicated rPET mixed with different fly ash loadings.

Table 4. Mix design of the fly ash–rPET waste composite material.

Designated Series	RP	RPF1	RPF2	RPF3	RPF4
Fly Ash (%)	0	23	42	58	68
rPET (%)	100	77	58	42	32

4.3. Extrusion Process

The extrusion process is a continuous processing technique in which a polymer material enhanced with the desired filler is melted and formed to improve the composite material characteristics of rPET [40,41,52,59–61]. This study focused on using a single-screw extruder (screw diameter—26 mm, L/D ratio—23, cylindrical die—13 mm Ø) described as follows:

→ Extruder temperature: 240 °C;
→ Die temperature: 260 °C;
→ Screw speed: 46 rpm.

The single-screw extruder machine with dimensions of 900 mm × 400 mm × 950 mm (i.e., width, depth, and high, respectively) was used for synthesising the composite material, as shown in Figure 7.

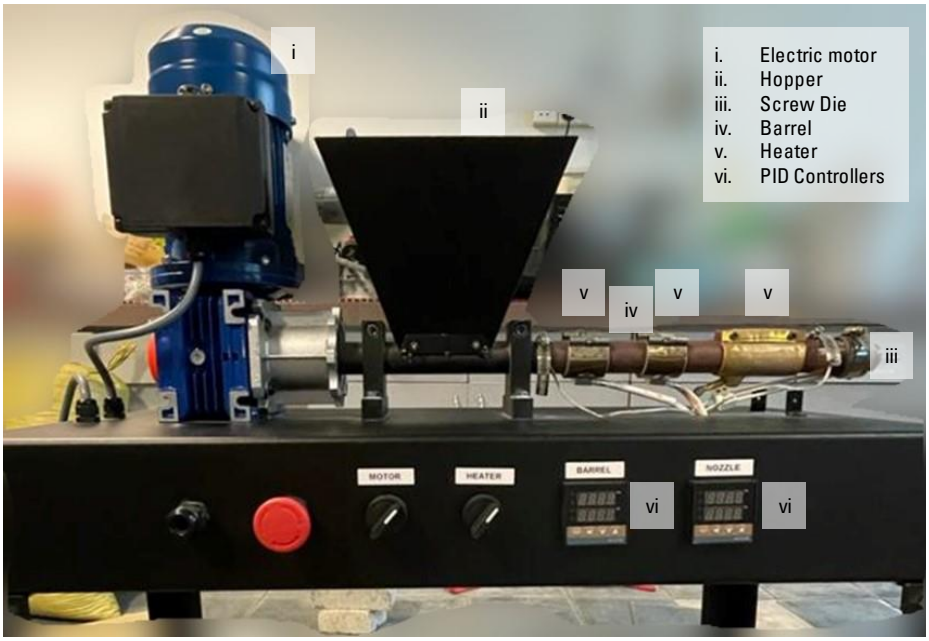

Figure 7. The single-screw extruder.

The pre-mixed rPET flakes and fly ash were gravity-fed into the hopper and dropped on a rotating screw via the feed throat. An electric motor drove the screw rotation. A schematic representation of the single-flighted stepped compression screw design is shown in Figure 8. The screw narrowed as the plastic passed through the barrel, compressing the plastic in the compressing zone. The barrel was heated by two independent proportional integral derivative PID controllers with a 5 × 220 V 250 W 35 × 50 heating band that created zones of gradually increasing temperature. Usually, the plastic melt temperature is higher than the temperature set for the controllers. This additional thermal energy was generated in the metering zone by combining compressive force and shear friction (shear heat).

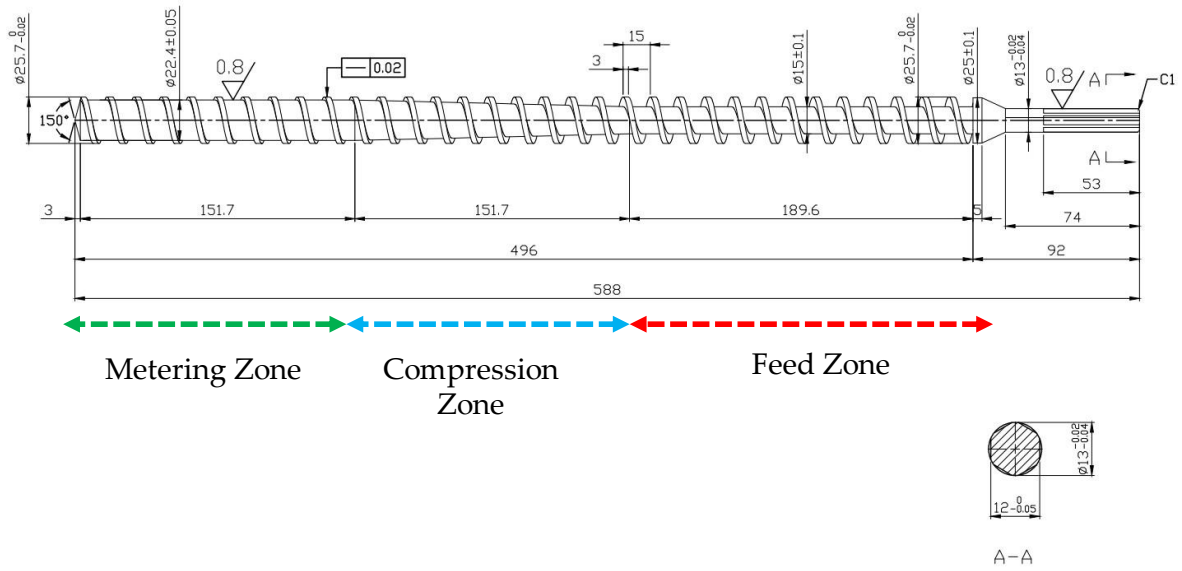

Figure 8. Diagram of single-flighted, stepped compression screw design and the mechanism zone.

When the plastic melt reached the screw's end, it was thoroughly mixed and pushed through the die. The extrudate was pulled and cooled at room temperature for 2 h after exiting the extruder. During the extrusion process, the extrudate composites flow out continuously, irrespective of the amount of pre-mixed rPET flakes and fly ash added into the hopper. However, the process will still result in the degradation of the composite material because only up to 300 g of the material can be successfully extruded and palletised for every 400 g of pre-mixed plastic flakes and fly ash added to the hopper. Almost 25% of the total composite material is allegedly lost or degraded during the extrusion process.

4.4. POST-Extrusion Process

After the extrusion process, the extruded material was pelletised into 1–10 mm granules, as shown in Figure 9, using a shredder machine. The colour of the composite material varies depending on its fly ash loading. In the absence of fly ash, the extruded rPET was pure white and exhibited a significant breakage rate during the pelletising procedure. When fly ash was added to the composite, the colour changed to greyish, and the breakage rate was reduced. The more fly ash present, the darker the colour. The colour of extruded composite with 68% fly ash was nearly black, and it was more rigid and difficult to break during the pelletising process. The breakage rate during the pelletisation process also affects the granule size. The granule size in 100% rPET with the highest breakage rate was 1–5 mm, while the composite of 68% fly ash with the lowest breakage rate was 3–8 mm.

4.5. Testing Method

Differential scanning calorimetry (DSC) was carried out with a DSC Q20 TA Instrument to analyse the glass transition temperature (T_g), crystallisation temperature (T_c), melting point temperature (T_m), and melting enthalpy (ΔH_m) for the composite material according to ASTM D3418-15. In the DSC method, an amount of plastic waste (range ~10 µg) is heated at a rate of 10 °C min^{-1} from 20 to 325 °C [38,39,62–65]. The crystallinity degree (Xc) was estimated using Equation (1) and a chosen enthalpy of 140 J/g for completely crystalline PET [64].

$$Xc\ (\%) = \Delta Hm/(\Delta H^{\circ}m) \times 100\% \quad (1)$$

where (ΔHm) is the melting enthalpy, and (ΔH°m) is the melting enthalpy of the 100% crystalline polymer [64].

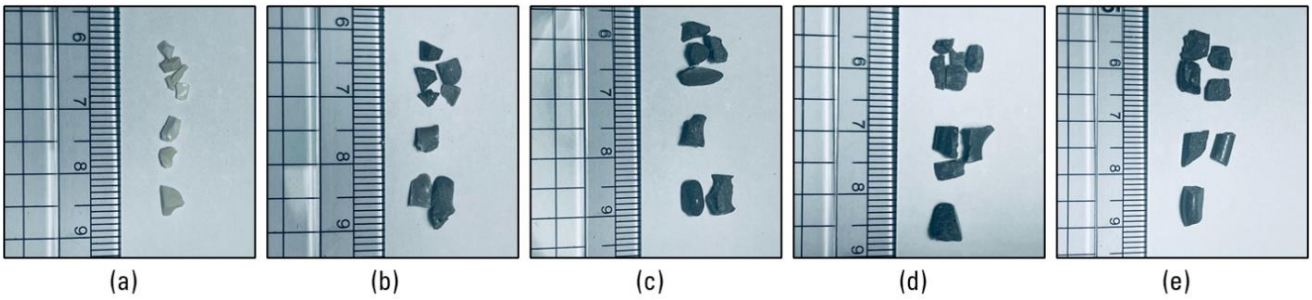

Figure 9. Visual appearance and justification of extruded composite material in granule form: (**a**) RP: extruded and shredded 100% rPET have a pure white colour and a granule size of 1–5 mm; (**b**) RPF1: extruded and shredded mixed rPET and fly ash have a light-greyish colour and a granule size of 3–7 mm; (**c**) RPF2: extruded and shredded mixed rPET and fly ash have a light-greyish colour a the granule size of 2–7 mm; (**d**) RPF3: extruded and shredded mixed rPET and fly ash have a dark-greyish colour and a granule size of 3–7 mm; (**e**) RPF4: extruded and shredded mixed rPET and fly ash have a dark-greyish colour and a granule size of 3–8 mm.

Scanning electron microscopy (SEM) with a JEOL model JSM-6010PLUS/LV (Joel, Tokyo, Japan) device equipped with an energy-dispersive X-ray (EDX) spectroscope (OXFORD Instrument, Abingdon, Oxfordshire) was used to examine the rPET blend, shape, and size of fly ash as well as the dispersion of fly ash within the polymer blends on the microscopic scale. The specimens' granule surfaces were sputter-coated with platinum before the morphologies of specimens were observed. The accelerating voltage used was 10 and 15 keV, respectively.

5. Conclusions

In this study, extruded recycled PET–fly ash composites were produced using a single-screw thread, and the effects of different fly ash loadings on their thermal behaviour and microstructure development were evaluated. DSC analysis revealed that adding fly ash as a filler to the rPET polymer matrix enhanced its crystalline properties, thereby improving the thermal behaviour of the composites. It was discovered that 58% fly ash loading resulted in the composite's highest glass transition temperature, melting temperature, and crystallisation temperature. Nonetheless, the composite's glass transition temperature, melting temperature, and crystallisation temperature decreased with increasing fly ash loading amounts, up to 68%. This can be explained by the fact that the effect decreases as a function of fly ash loading, indicating a progressive deterioration of fly ash dispersion, as evidenced by fly ash agglomerates in SEM images. Further research on developing composite material rPET and fly ash will be focused on evaluating the mechanical properties. Other factors, such as filler treatment and matrix compatibiliser, will be included. Likewise, this improved composite material will be used in subsequent studies to support its use as an alternative construction material.

Author Contributions: Conceptualisation, N.H.M.N. and F.U.; methodology, N.H.M.N., F.U. and M.N.M.A.; validation, F.U., E.L.W. and M.N.M.A.; writing—original draft preparation, N.H.M.N.; writing—review and editing, N.H.M.N., F.U., E.L.W., A.B.M.S. and S.; supervision, F.U. and E.L.W. All authors have read and agreed to the published version of the manuscript.

Funding: This research was funded by IRMC UNITEN BOLDREFRESH2025-CENTRE OF EXCELLENCE. THE APC was funded by IRMC UNITEN.

Data Availability Statement: Not applicable.

Acknowledgments: The authors are grateful to acknowledge the IRMC UNITEN and the Institute of Energy Infrastructure (IEI) for the lab facilities and financial support provided through BOLD 2021 research grant.

Conflicts of Interest: The authors declare no conflict of interest.

References

1. Plastic Soup Foundation. Plastics Facts & Figures. 2019. Available online: https://www.plasticsoupfoundation.org/en/plastic-facts-and-figures/ (accessed on 20 April 2022).
2. European Association of Plastic Recycling. *Plastics—The Facts 2021*; European Association of Plastic Recycling: Woluwe Saint-Pierre, Brussels, 2021.
3. Fuhr, L. *Plastic Atlas Second Edition*; Heinrich Böll Foundation: Berlin, Germany, 2019.
4. Ncube, L.K.; Ude, A.U.; Ogunmuyiwa, E.N.; Zulkifli, R.; Beas, I.N. An Overview of Plastic Waste Generation and Management in Food Packaging Industries. *Recycling* **2021**, *6*, 12. [CrossRef]
5. Kumartasli, S.; Avinc, O. Important Step in Sustainability: Polyethylene Terephthalate Recycling and the Recent Developments. In *Sustainability in the Textile and Apparel Industries*; Springer: Berlin/Heidelberg, Germany, 2020. [CrossRef]
6. Sharma, S.; Sudhakara, P.; Misra, S.; Singh, J. A comprehensive review of current developments on the waste-reinforced polymer-matrix composites for automotive, sports goods and construction applications: Materials, processes and properties. *Mater. Today Proc.* **2020**, *33*, 1671–1679. [CrossRef]
7. Kumar, A.; Bedi, R.; Singh, B. Composite materials based on recycled polyethylene terephthalate and their properties—A comprehensive review. *Compos. B Eng.* **2021**, *219*, 108928.
8. Golden Ecosystem. *A Study on Plastic Management in Peninsular Malaysia*; National Solid Waste Management Department, Ministry of Housing and Local Government Malaysia: Putrajaya, Malaysia, 2011.
9. Sarioğlu, E.; Kaynak, H.K. *PET Bottle Recycling for Sustainable Textiles*; IntechOpen: London, UK, 2018. [CrossRef]
10. Siddique, R.; Khatib, J.; Kaur, I. Use of recycled plastic in concrete: A review. *Waste Manag.* **2008**, *28*, 1835–1852. [CrossRef]
11. Tiseo, I. Global Production Capacity of Polyethylene Terephthalate 2014–2024. Statistica, 2021. Available online: https://www.statista.com/statistics/242764/global-polyethylene-terephthalate-production-capacity/ (accessed on 21 April 2022).
12. Awaja, F.; Pavel, D. Recycling of PET. *Eur. Polym. J.* **2005**, *41*, 1453–1477. [CrossRef]
13. Selvaraj, V.; Raghavarshini, T.R.; Alagar, M. Development of *Prosopis juliflora* carbon-reinforced PET bottle waste-based epoxy-blended bio-phenolic benzoxazine composites for advanced applications. *RSC Adv.* **2020**, *10*, 5656–5665. [CrossRef]
14. Paszun, D.; Spychaj, T. Chemical Recycling of Poly(ethylene terephthalate). *Ind. Eng. Chem. Res.* **1997**, *36*, 1373–1383. [CrossRef]
15. Khoramnejadian, S. Enhance mechanical and thermal properties of recycled Poly ethylene terephetalat (PET) from used bottle. *Adv. Environ. Biol.* **2011**, *5*, 3826–3829.
16. Cazan, C.; Cosnita, M.; Visa, M.; Duta, A. Novel rubber—Plastics composites fully based on recycled materials. In *Sustainable Energy in the Built Environment-Steps Towards nZEB*; Springer: Berlin/Heidelberg, Germany, 2014; pp. 503–519. [CrossRef]
17. Geyer, B.; Lorenz, G.; Kandelbauer, A. Recycling of poly(ethylene terephthalate)—A review focusing on chemical methods. *Express Polym. Lett.* **2016**, *10*, 559–586. [CrossRef]
18. Singh, A.K.; Bedi, R.; Kaith, B.S. Mechanical properties of composite materials based on waste plastic—A review. *Mater. Today Proc.* **2019**, *26*, 1293–1301. [CrossRef]
19. Sharifian, S.; Asasian-Kolur, N. Polyethylene terephthalate (PET) waste to carbon materials: Theory, methods and applications. *J. Anal. Appl. Pyrolysis* **2022**, *163*, 105496. [CrossRef]
20. U.S. Energy Information Administration. *Country Analysis Executive Summary: Malaysia*; U.S. Energy Information Administration: Washington, DC, USA, 2021.
21. Suruhanjaya Tenaga Energy Commision. *National Energy Balance 2019*; Suruhanjaya Tenaga Energy Commision: Putrajaya, Malaysia, 2022.
22. Delos Reyes, A. Indonesia, Malaysia's TNB Agree Coal Supply Deal, Argusmedia, 2022. Available online: https://www.argusmedia.com/pt/news/2336699-indonesia-malaysias-tnb-agree-coal-supply-deal (accessed on 22 August 2022).
23. Fong, N. Rise of Coal in Malaysia, Macaranga, 2021. Available online: https://www.macaranga.org/coal-statistics-malaysia/ (accessed on 22 August 2022).
24. Fauzi, A.; Nuruddin, M.F.; Malkawi, A.B.; Abdullah, M.M.A.B. Study of Fly Ash Characterization as a Cementitious Material. *Procedia Eng.* **2016**, *148*, 487–493. [CrossRef]
25. *ASTM C618-19*; Standard Specification for Coal Fly Ash and Raw or Calcined Natural Pozzolan for Use. ASTM International: West Conshohocken, PA, USA, 2019.
26. Nordin, N.; Mustafa, M.; Bakri, A. Utilisation of fly ash waste as construction material. *Int. J. Conserv. Sci.* **2016**, *7*, 161–166.
27. Ghazali, N.; Muthusamy, K.; Ahmad, S.W. Utilization of fly ash in construction. In Proceedings of the IOP Conference Series: Materials Science and Engineering; IOP Publishing: Bristol, UK, 2019; Volume 601, p. 012023.
28. Bhatt, A.; Priyadarshini, S.; Mohanakrishnan, A.A.; Abri, A.; Sattler, M.; Techapaphawit, S. Physical, chemical, and geotechnical properties of coal fly ash: A global review. *Case Stud. Constr. Mater.* **2019**, *11*, e00263. [CrossRef]
29. Devi, M.S.; Murugesan, V.; Rengaraj, K.; Anand, P. Utilisation of flyash as filler for unsaturated polyester resin. *J. Appl. Polym. Sci.* **1998**, *69*, 1385–1391. [CrossRef]
30. Gohatre, O.K.; Biswal, M.; Mohanty, S.; Nayak, S.K. Study on thermal, mechanical and morphological properties of recycled poly(vinyl chloride)/fly ash composites. *Polym. Int.* **2020**, *69*, 552–563. [CrossRef]
31. Kasar, A.K.; Gupta, N.; Rohatgi, P.K.; Menezes, P.L. A Brief Review of Fly Ash as Reinforcement for Composites with Improved Mechanical and Tribological Properties. *J. Miner. Met. Mater. Soc.* **2020**, *72*, 2340–2351. [CrossRef]

32. Yang, Y.-F.; Gai, G.-S.; Cai, Z.-F.; Chen, Q.-R. Surface modification of purified fly ash and application in polymer. *J. Hazard. Mater.* **2006**, *133*, 276–282. [CrossRef]
33. Bicer, A. Effect of fly ash particle size on thermal and mechanical properties of fly ash-cement composites. *Therm. Sci. Eng. Prog.* **2018**, *8*, 78–82. [CrossRef]
34. Babu, D.S.; Babu, K.G.; Wee, T. Properties of lightweight expanded polystyrene aggregate concretes containing fly ash. *Cem. Concr. Res.* **2005**, *35*, 1218–1223. [CrossRef]
35. Alkan, C.; Arslan, M.; Cici, M.; Kaya, M.; Aksoy, M. A study on the production of a new material from fly ash and polyethylene. *Resour. Conserv. Recycl.* **1995**, *13*, 147–154. [CrossRef]
36. Li, Y.; White, D.J.; Peyton, R.L. Composite material from fly ash and post-consumer PET. *Resour. Conserv. Recycl.* **1998**, *24*, 87–93. [CrossRef]
37. Liu, S.-J. *Recycled Plastics as Fillers in Polymer Cement Concrete Composites*; New Jersey Institute of Technology: Newark, NJ, USA, 1988.
38. White, D.J. Microstructure of Composite Material from High-Lime Fly Ash and RPET. *J. Mater. Civ. Eng.* **2000**, *12*, 60–65. [CrossRef]
39. Rebeiz, K.S.; Banko, A.S.; Craft, A.P. Thermal Properties of Polymer Mortar Using Recycled PET and Fly Ash. *J. Mater. Civ. Eng.* **1995**, *7*, 129–133. [CrossRef]
40. Sharma, A.K.; Mahanwar, P.A. Effect of particle size of fly ash on recycled poly (ethylene terephthalate)/fly ash composites. *Int. J. Plast. Technol.* **2010**, *14*, 53–64. [CrossRef]
41. Joseph, P.A.M.S.; Bambola, V.A.; Sherhtukade, V.V. Effect of flyash content, particle size of flyash, and type of silane coupling agents on the properties of recycled poly(ethylene terephthalate)/flyash composite. *J. Appl. Polym. Sci.* **2010**, *115*, 201–208. [CrossRef]
42. De Pardo, P.S.G.; Bernal, C.; Ares, A.; Abad, M.; Cano, J. Rheological, thermal, and mechanical characterisation of fly ash-thermoplastic composites with different coupling agents. *Polym. Polym. Compos.* **2010**, *16*, 101–113. [CrossRef]
43. Dhawan, R.; Bisht, B.M.S.; Kumar, R.; Kumari, S.; Dhawan, S. Recycling of plastic waste into tiles with reduced flammability and improved tensile strength. *Process. Saf. Environ. Prot.* **2019**, *124*, 299–307. [CrossRef]
44. Singh, G.; Kumar, H.; Singh, S. Performance evaluation-PET resin composite composed of red mud, fly ash and silica fume. *Constr. Build. Mater.* **2019**, *214*, 527–538. [CrossRef]
45. Garbacz, A.; Sokołowska, J.J. Concrete-like polymer composites with fly ashes—Comparative study. *Constr. Build. Mater.* **2013**, *38*, 689–699. [CrossRef]
46. Satapathy, S.; Nag, A.; Nando, G.B. Thermoplastic elastomers from waste polyethylene and reclaim rubber blends and their composites with fly ash. *Process. Saf. Environ. Prot.* **2010**, *88*, 131–141. [CrossRef]
47. Gaval, V.R.; Sahai, R.S.N. Effect of particle size and concentration of fly ash on properties of polytrimethylene terepthalate. In Proceedings of the 2015 International Conference on Chemical, Metallurgy and Material Science Engineering, Pattaya, Thailand, 10–11 August 2015; pp. 46–51.
48. Sreekanth, M.; Bambole, V.; Mhaske, S.; Mahanwar, P. Effect of Particle Size and Concentration of Flyash on Properties of Polyester Thermoplastic Elastomer Composites. *J. Miner. Mater. Charact. Eng.* **2009**, *8*, 237–248. [CrossRef]
49. Nasir, N.H.M.; Usman, F.; Saggaf, A.; Saloma. Development of composite material from Recycled Polyethylene Terephthalate and fly ash: Four decades progress review. *Curr. Res. Green Sustain. Chem.* **2022**, *5*, 100280. [CrossRef]
50. Chen, S.; Xie, S.; Guang, S.; Bao, J.; Zhang, X. Crystallisation and Thermal Behaviors of Poly(ethylene tereph-thalate)/Bisphenols Complexes through Melt Post-Polycondensation. *Polymers* **2020**, *12*, 3053. [CrossRef]
51. Fa, D.; Huang, S.K.; Lee, J. DSC Studies on the Crystallisation Characteristics of Poly(Ethylene Terephthalate) for Blow Molding Applications. *Polym. Eng. Sci.* **1998**, *3*, 2.
52. Mohsin, M.A.; Abdulrehman, T.; Haik, Y. Reactive Extrusion of Polyethylene Terephthalate Waste and Investigation of Its Thermal and Mechanical Properties after Treatment. *Int. J. Chem. Eng.* **2017**, *2017*, 15–18. [CrossRef]
53. Deepthi, M.; Sharma, M.; Sailaja, R.; Anantha, P.; Sampathkumaran, P.; Seetharamu, S. Mechanical and thermal characteristics of high density polyethylene–fly ash Cenospheres composites. *Mater. Des.* **2010**, *31*, 2051–2060. [CrossRef]
54. Morawiec, J.; Galeski, A. Characterisation of scrap poly (ethylene terephthalate). *Eur. Polym. J.* **2000**, *36*, 1875–1884.
55. Torres, N.; Robin, J.; Boutevin, B. Study of thermal and mechanical properties of virgin and recycled poly(ethylene terephthalate) before and after injection molding. *Eur. Polym. J.* **2000**, *36*, 2075–2080. [CrossRef]
56. Miandad, R.; Rehan, M.; Barakat, M.A.; Aburiazaiza, A.S.; Khan, H.; Ismail, I.M.I.; Dhavamani, J.; Gardy, J.; Hassanpour, A.; Nizami, A.-S. Catalytic Pyrolysis of Plastic Waste: Moving Toward Pyrolysis Based Biorefineries. *Front. Energy Res.* **2019**, *7*, 92–108. [CrossRef]
57. Hahladakis, J.N.; Velis, C.A.; Weber, R.; Iacovidou, E.; Purnell, P. An overview of chemical additives present in plastics: Migration, release, fate and environmental impact during their use, disposal and recycling. *J. Hazard. Mater.* **2018**, *344*, 179–199. [CrossRef] [PubMed]
58. Cotto-Ramos, A.; Dávila, S.; Torres-García, W.; Cáceres-Fernández, A. Experimental design of concrete mixtures using recycled plastic, fly ash, and silica nanoparticles. *Constr. Build. Mater.* **2020**, *254*, 119207. [CrossRef]
59. Carbassi, F.; Messina, G.; Guido, I.; Enichem, D.; Fauser, V.G. Chain Extension of Recycled Poly (ethylene terephthalate). *J. Appl. Polym. Sci.* **1993**, *50*, 1501–1509. [CrossRef]

60. Incarnato, L.; Scarfato, P.; di Maio, L.; Acierno, D. Structure and rheology of recycled PET modified by reactive extrusion. *Polymer* **2000**, *41*, 6825–6831. [CrossRef]
61. Jayanarayanan, K.; Thomas, S.; Joseph, K. In situ microfibrillar blends and composites of polypropylene and poly (ethylene terephthalate): Morphology and thermal properties. *J. Polym. Res.* **2011**, *18*, 1–11. [CrossRef]
62. Badía, J.; Vilaplana, F.; Karlsson, S.; Ribes-Greus, A. Thermal analysis as a quality tool for assessing the influence of thermo-mechanical degradation on recycled poly(ethylene terephthalate). *Polym. Test.* **2009**, *28*, 169–175. [CrossRef]
63. Kuzmanović, M.; Delva, L.; Cardon, L.; Ragaert, K. The Effect of Injection Molding Temperature on the Morphology and Mechanical Properties of PP/PET Blends and Microfibrillar Composites. *Polymers* **2016**, *8*, 13–18. [CrossRef] [PubMed]
64. Van Kets, K.; Delva, L.; Ragaert, K. Structural stabilizing effect of SEBSgMAH on a PP-PET blend for multiple mechanical recycling. *Polym. Degrad. Stab.* **2019**, *166*, 60–72. [CrossRef]
65. Asensio, M.; Nuñez, K.; Guerrero, J.; Herrero, M.; Merino, J.; Pastor, J. Rheological modification of recycled poly(ethylene terephthalate): Blending and reactive extrusion. *Polym. Degrad. Stab.* **2020**, *179*, 109258. [CrossRef]